scientific reports

Check for updates

OPEN

LncRNA-Gm17586 inhibits *S.typhimurium* mediated pyroptosis by promoting NLRP3 and Tnip1 binding

Zhiyuan An[1]✉ & Wenyi Ding[2]

The aim of this study is to identify the lncRNA that directly interacts with NLRP3 molecules in RAW264.7 cells infected with *S. typhimurium* and its role in *S. typhimurium*-mediated pyroptosis. We have identified LncRNA-Gm17586, which directly interacts with NLRP3 in RAW264.7 cells infected with *S. typhimurium*. LncRNA-Gm17586 inhibits *S. typhimurium*-mediated pyroptosis in RAW264.7 cells. Overexpression of LncRNA-Gm17586 not only directly suppresses NLRP3 inflammasome activation but also enhances the binding affinity between Tnip1 and NLRP3, thereby indirectly facilitating Tnip1-mediated inhibition of the NLRP3 inflammasome. Consequently, this dual mechanism effectively inhibits *S. typhimurium*-induced pyroptosis. Our results demonstrate that LncRNA-Gm17586 directly interacts with NLRP3 during *S. typhimurium*-mediated pyroptosis and inhibits this process by enhancing the interaction between Tnip1 and NLRP3.

Keywords LncRNA-Gm17586, Pyroptosis, *S.typhimurium*, Tnip1, RIP-seq

Salmonella enterica serovar Typhimurium (*S.Typhimurium*) is a non-specific zoonotic bacterium capable of causing infections in both humans and animals, leading to acute intestinal inflammation and foodborne illness. It is recognized as a significant foodborne pathogen prevalent across various regions globally. In recent years, the emergence of multidrug-resistant *S. Typhimurium* has resulted in numerous public health crises worldwide. Research has demonstrated that *S. Typhimurium* exhibits high invasiveness, with its type III secretion system facilitating invasion into host intestinal epithelial cells, entry into systemic circulation, or survival and replication within macrophages. This pathogenic capability is closely associated with virulence factors[1,2]. The innate immune system serves as the first line of defense against pathogenic infections, exemplified by extracellular Toll-like receptors (TLRs) and intracellular NOD-like receptors (NLRs). The virulence factors secreted by *S. Typhimurium*, along with its type III secretion system, can adapt to, manipulate, and disrupt these pattern recognition receptors, thereby enabling successful survival strategies within host cells[3].

NLRP3 inflammasomes are critical pattern recognition receptors (PRRs) within the host innate immune system, responsible for detecting pathogen-associated molecular patterns (PAMPs) and danger-associated molecular patterns (DAMPs). Extensive research has demonstrated that NLRP3 inflammasomes play a pivotal role not only in infectious diseases caused by bacteria and viruses but also in non-alcoholic steatohepatitis (NASH), inflammatory bowel disease, neurodegenerative disorders, and various types of cancer[4-9]. The activation of the NLRP3 inflammasome is a two-step process, comprising an initiation phase and an activation phase. During the initiation phase, Toll-like receptors (TLRs) recognize PAMPs and DAMPs, leading to the activation of NF-κB, which upregulates the transcription of NLRP3, pro-caspase-1, and pro-IL-1β. In the subsequent activation phase, intracellular potassium efflux and mitochondrial dysfunction induce conformational changes in NLRP3. The N-terminal pyrin domain (PYD) of NLRP3 interacts with apoptosis-associated speck-like protein containing a CARD (ASC), which also possesses a PYD domain, forming ASC specks. This interaction facilitates the recruitment of pro-caspase-1 via its caspase recruitment domain (CARD), resulting in caspase-1 activation and the cleavage of pro-IL-1β into mature IL-1β. Activated caspase-1 further cleaves Gasdermin D (GSDMD) into its N-terminal fragment (GSDMD-N), which translocates to the cell membrane to form pores, facilitating the release of IL-1β and inducing pyroptosis[10]. Numerous studies have shown that *S. typhimurium* invasion of

[1]Medical Research Center, Beijing Chaoyang Hospital, Capital Medical University, Beijing 100020, China. [2]Department of Clinical Laboratory, Peking Union Medical College Hospital, Chinese Academy of Medical Sciences, Beijing 100730, China. ✉email: mran850712@aliyun.com

host cells activates both NLRC4 and NLRP3 inflammasomes through its flagella and type III secretion systems, leading to pyroptosis and subsequent host inflammatory responses[11-13].

Long non-coding RNAs (lncRNAs) are non-coding RNA molecules with a length exceeding 200 nucleotides. They play extensive regulatory roles in epigenetics, pre- and post-transcriptional regulation, DNA synthesis, and various physiological and pathological processes[14-16]. Recent studies have demonstrated that multiple lncRNAs significantly influence the regulation of cardiovascular diseases, metabolic disorders, and infectious diseases mediated by NLRP3-driven innate immune responses, potentially serving as therapeutic targets[17-19]. For instance, Niu et al. found that LncRNA-KCNQ1OT1 promotes hepatitis C virus-induced infection by mediating the miRNA-223-3p/NLRP3 axis in β-cell pyroptosis. Deng et al. reported that *Brucella* downregulates LncRNA-Gm28309 via the miR-3068-5p/NF-κB pathway, thereby triggering a macrophage inflammatory response. These findings suggest that pathogen infections modulate host cell lncRNA expression, leading to pyroptosis[20,21]. Additionally, recent research has shown that certain anti-inflammatory drugs can regulate lncRNA expression and facilitate the clearance of *S. typhimurium* infection in mice[22,23]. However, there is currently limited research on the changes in lncRNA expression caused by *S. typhimurium* infection in host cells and how these changes affect pyroptosis.

This study aims to employ RIP-seq technology to identify differentially expressed lncRNAs that directly interact with NLRP3 molecules in RAW264.7 cells, both infected and uninfected with *S. typhimurium*. Subsequently, we will focus on the lncRNA exhibiting the most significant expression difference between the infected and uninfected groups to further investigate its role in NLRP3 activation and *S. typhimurium*-mediated pyroptosis.

Materials and methods

Cell culture

The mouse macrophage cell line, RAW264.7, (ATCC®TIB-71) was obtained from the American Type Culture Collection (ATCC). RAW264.7 cells were cultured in DMEM supplemented with 10% fetal bovine serum (FBS) and antibiotics, in a humidified atmosphere with 5% CO2 at 37 °C.

RIP-seq

RNA immunoprecipitation (RIP) was performed using the EZ-Magna RIP Kit (Millipore, Burlington, MA, United States) according to the manufacturer's protocol. Briefly, after 4 h of *S. typhimurium* infection in RAW264.7 cells, lysis buffer was used to prepare cell lysates. A monoclonal antibody against NLRP3 was added to the lysate and co-precipitated with protein A/G magnetic beads overnight. The following day, protease K was used to remove proteins, and total RNA was extracted using a phenol:chloroform:isoamyl alcohol mixture (125:24:1, pH 4.3). The integrity and concentration of the purified RNA were assessed using a Nanodrop (US). Sequencing was performed on an Illumina NovaSeq 6000 platform. Data analysis was conducted using the following software tools: Solexa pipeline version 1.8 for image processing and base recognition, FastQC for quality control of sequencing reads, Hisat2 for alignment to reference genomes, StringTie for estimating transcription abundance based on official database annotations, and R software (Ballgohan package) for FPKM calculations at the gene and transcript levels to identify differentially expressed genes. All experiments were independently repeated three times. The above work was carried out by Kangchen Biotechnology (Shanghai, China), and the sequencing data were deposited in the National Center for Biotechnology Information Gene Expression Omnibus (GEO) database under accession number GSE250407. Heatmaps and volcano plots were generated using OmicStudio tools available at https://www.omicstudio.cn.

Western blot analysis

Cell lysates were prepared using 5 × sodium dodecyl sulfate (SDS) sample buffer. Proteins were separated on 10% SDS-PAGE gels and transferred onto polyvinylidene fluoride (PVDF) membranes (Millipore, USA). Membranes were then incubated with the following primary antibodies against GAPDH(1:1000; Cell Signaling Technology, #5174), NLRP3 (1:1000; AdipoGen, AG-20B-0014), caspase-1/p20 (1:1000; Proteintech, 22,915–1-AP), GSDMD/p30 (1:1000; Affinity Biosciences, AF-4012), and Tnip1(1:1000; Proteintech, 15,104–1-AP). Immunoblotting markers were purchased from Thermo (#26,616). Band intensity was quantified using ImageJ software (NIH, Bethesda, MD, USA). All experiments were independently repeated three times.

Florescence in situ *hybridization and immunofluorescence*

RAW264.7 cells were then fixed with 4% paraformaldehyde for 15 min. The cells were then permeabilized with 0.3% Triton X100 for 10 min. The cells were then washed with PBS three times, and incubated with Tnip1 and NLRP3 monoclonal antibodies at 37 °C for 2 h. The samples were mixed with goat anti-mouse fluorescent secondary antibodies and incubated at room temperature for 1 h. The nuclei were stained with DAPI, and images were acquired using an Olympus X51 fluorescence microscope (objective, 40X). LncRNA-Gm17586 fluorescence staining was performed according to the instructions of the RNA-FISH kit (Genepharma, Suzhou, China), and the results were observed using an Olympus X51 fluorescence microscope. All experiments was independently repeated thrice.

Lentivirus construction

Lentivirus-Gm17586 (LV-Gm17586-fluorescent and LV-Gm17586-non-fluorescent) and Lentivirus-Tnip1 (LV-Tnip1) were constructed by Genepharma (Shanghai, China). The specific preparation steps are as follows: Prepare the recombinant viral plasmid encoding the target gene along with its three auxiliary packaging components: pGag/Pol, pRev, and pVSV-G vector plasmids. Perform high-purity, endotoxin-free extraction of the plasmids. Co-transfect 293 T cells with the RNAi Mate transfection reagent using the prepared plasmids. After 6 h of

transfection, replace the culture medium with complete medium. After an additional 72 h of cultivation, collect the cell supernatant rich in lentiviral particles. Concentrate the collected supernatant to obtain a high-titer lentiviral concentrate for infecting the target cells.

Real-time PCR

Cells were seeded in six-well plates and cultured. Total RNA was extracted from the cultured cells using TRIzol reagent (Invitrogen, Carlsbad, CA, USA) according to the manufacturer's protocol. First-strand cDNA was synthesized using the First-Strand cDNA Synthesis SuperMix and TransScript Green miRNA Two-Step qRT-PCR SuperMix (TransGen Biotech Co., Ltd.) following the manufacturer's instructions. GAPDH was used as an endogenous control. The qPCR reaction system consisted of 0.4 μL of forward primer, 0.4 μL of reverse primer, 10 μL of 2 × Perfect StartTM Green qPCR SuperMix, 0.4 μL of Passive Reference Dye, 1 μL of cDNA template, and ddH2O added to a final volume of 20 μL. The thermal cycling conditions were as follows: 94 °C for 30 s, followed by 40 cycles of 94 °C for 5 s, 55 °C for 15 s, and 72 °C for 10 s. Gene expression levels were quantified using the 2^(-ΔΔCt) method. The region-specific primers used are listed in Table 1. All experiments were independently repeated three times.

LDH release assay

To analyze intracellular injury associated with pyroptotic cell death, LDH release was measured using the LDH Cytotoxicity Assay Kit (Beyotime Biotechnology, C0017) according to the manufacturer's instructions. Absorbance was recorded at 490 nm using a microplate reader (Tecan, Salzburg, Austria). All experiments were independently repeated three times.

ELISA assay

RAW264.7 cells were infected with LV-Gm17586 at an MOI of 100 for 72 h, followed by infection with *S. typhimurium* at an MOI of 20 for 4 h. The cell culture supernatant was collected and analyzed using a mouse IL-1β ELISA kit (Thermo Fisher, KMC0011) according to the manufacturer's instructions. Absorbance was measured at 450 nm using a microplate reader (Tecan). All experiments were independently repeated three times.

LC–MS spectrometry

The analysis was performed using a nano liquid chromatograph (Waters nanoEquity HPLC) coupled with a high-resolution mass spectrometer (Thermo Orbitrap Fusion Lumos with nano spray ESI source). The sample preparation steps were as follows: Add 100 μL of a 3:7 acetonitrile and 100 mM ABC solution to decolorize the colloidal particles. Dehydrate the colloidal particles by adding acetonitrile until they turn white. Add 100 μL of 10 mM DTT and incubate at room temperature for 30 min. Incubate with 100 μL of IAM (containing 50 mM ABC) and 55 mM IAM in the dark at room temperature for 30 min. Add an appropriate amount of

Gene	Primer	Sequence(5′-3′)
Gm28875	forward reverse	ACCTCCCCTTGTCACAGTCT CAGGACTCACTTGGCCCTTC
Gm17586	forward reverse	GGTTTTCCACTTTGGTGGGTC GGGGCTTGTTCCAGTATGGG
Gm10825	forward reverse	AAGTGTCCACATCCTACCAGT ACCGTGGGCATCAACTGTAA
Gm28399	forward reverse	AGCTTCGGGGACTTCCTCTC CCAGCCATCCCCTTTCCTAAC
Gm26581	forward reverse	ACCACAGAGACTCCCGACAAT AAGAGGTGAGGATTCTGTGCC
9030407P20Rik	forward reverse	TTTGGGATGCCTACATGTCC CCAATCTACGTGGTGGCACT
2900097C17Rik	forward reverse	TCGTTGTCTTTGGGGAGTGG ACACACACTACATGGCCGTT
B230354K17Rik	forward reverse	GATGCCGGACGGACTCAAG AGGAAGGAGAGCGAACACTT
Gm20632	forward reverse	TCACGAAAGCGCAAACAGAC GCAAATGAAGCCACCGAGC
AC117245.1	forward reverse	GAGGACGAATTCCAGACGCT CCTCCCAGATTCCAAACGGA
AC117245.2	forward reverse	GCCCAAGCCAGAAGAGTGAC TCAAATTCCCCATGTGTGGGT
Gm14636	forward reverse	GCAGTGTTGAAGCCGAAAGC AACGGCTTTGTTCTGATCGC
Gm43069	forward reverse	GGCTTCCTGACCTCCTATTTGG TGAGAACTTGGGTGGGGAGG
Actin	forward reverse	CATTGCTGACAGGATGCAGAAGG TGCTGGAAGGTGGACAGTGAGG

Table 1. The primers listed in table 1 are qPCR amplification primers for differentially expressed lncRNA.

acetonitrile to completely dry the colloidal particles. Add 20 µL of enzyme solution diluted in 50 mM ABC + 5% acetonitrile to the dried colloidal particles. Incubate overnight at 37 °C in a protective solution (5% acetonitrile, 25 mM ABC). Transfer the supernatant after enzymatic hydrolysis into a centrifuge tube, add 30% acetonitrile and 0.1% formic acid, and shake for 30 min. Mix the supernatant with enzyme-hydrolyzed supernatant and repeat the process using 60% acetonitrile and 0.1% formic acid. Concentrate and extract the solution using a centrifugal concentrator. Dissolve the sample again in 0.1% formic acid aqueous solution and adjust the total volume to between 10–20 µL for mass spectrometry analysis. The resulting samples were analyzed using the mass spectrometer. Database searches were conducted using Peaks software (version 2.0.1.0) to obtain the final results.

Statistical analysis

Statistical analyses were performed using two-tailed Student's *t*-test. Data are presented as mean ± standard error of the mean [SEM]). Significant differences were defined to p-values < 0.05 or < 0.01 (denoted by* or ** and # or ##, respectively).

Result

Identification of LncRNAs Directly Interacting with NLRP3 in S. typhimurium-Infected RAW264.7 Cells

We employed RIP-seq technology to identify lncRNAs that directly interact with NLRP3 molecules in sequencing experiments. The sequencing results revealed that, compared to the uninfected group, infection of RAW264.7 cells with *S. typhimurium* for 4 h led to a significant decrease in the expression of nine lncRNAs: LncRNA-Gm28875, Gm17586, Gm10825, Gm38399, Gm26581, Gm20362, 9030407P20Rik, 2900097C17Rik, and B230354K17Rik. Conversely, the expression of four lncRNAs: AC117245.1Rik, AC117245.2Rik, Gm14636, and Gm43069 were significantly increased. These findings are illustrated in heatmaps and volcano plots, with fold changes (FC) greater than 2 and p-values less than 0.05 (Fig. 1A and 1B).

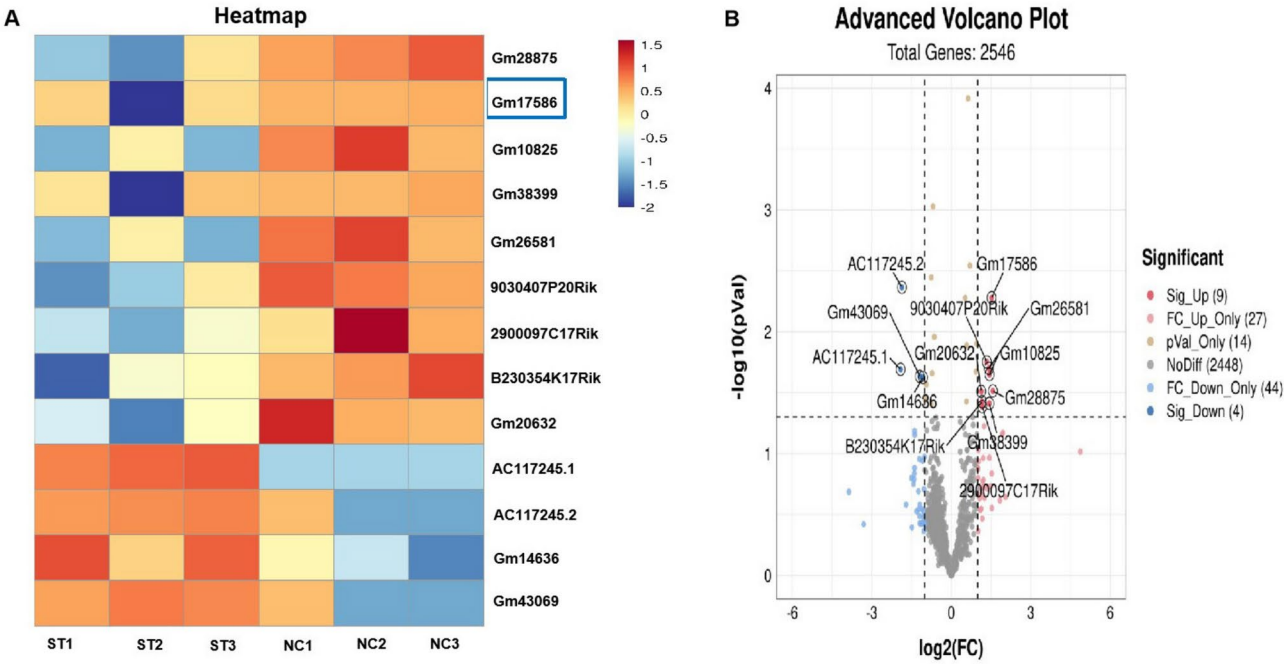

Fig. 1. **Identification of LncRNAs Directly Interacting with NLRP3 in S. typhimurium-Infected RAW264.7 Cells** (**A**): After infecting RAW264.7 cells with *S.typhimurium* for 4 h, lncRNAs exhibiting significant differential expression compared to the uninfected group were identified using RIP-seq. Subsequently, bioinformatics analysis was performed to analyze the differential expression of lncRNAs, and the results were visualized as heatmaps (FC > 2, p < 0.05). In the figure, "ST" denotes the *S.typhimurium* infection group, while "NC" represents the uninfected control group. Each experiment was independently repeated three times. (**B**): Following a 4-h infection of RAW264.7 cells with *S.typhimurium*, lncRNAs showing significant differential expression relative to the uninfected group were detected using RIP-seq. Bioinformatics analysis was then conducted to assess the differential expression of lncRNAs, and the results were presented as a volcano plot (FC > 2, p < 0.05). The figure illustrates the comparison between the uninfected and infected groups. Each experiment was independently repeated three times.

Validation of Sequencing Results and Subcellular Localization Detection of LncRNA-Gm17586

To validate the sequencing results, we performed qPCR to assess the expression levels of the identified lncRNAs. The qPCR results confirmed that the nine downregulated lncRNAs exhibited significantly lower expression in the infected group compared to the uninfected group (*$p < 0.05$), consistent with the sequencing data. Specifically, the p-values for LncRNA-Gm17586, Gm38399, and B230354K17Rik were 0.00526, 0.03875, and 0.03739, respectively, indicating that LncRNA-Gm17586 was the most significantly reduced among these lncRNAs. Therefore, based on both the sequencing and qPCR results, we selected LncRNA-Gm17586 as the focus of our study. Additionally, there were no statistically significant changes in the expression of AC117245.1Rik, AC117245.2Rik, Gm14636, or Gm43069 (Fig. 2A). Furthermore, time-course experiments demonstrated that prolonged infection of RAW264.7 cells with *S. typhimurium* led to a progressive reduction in LncRNA-Gm17586 expression. Compared to the uninfected group, expression decreased by 16 h of infection (*$p < 0.05$, **$p < 0.01$; Fig. 2B). To investigate the subcellular localization of LncRNA-Gm17586, we separated the nucleus and cytoplasm from RAW264.7 cells and detected its expression using qPCR. The results indicated that LncRNA-Gm17586 was predominantly expressed in the cytoplasm (97.5%), with only 2.5% localized in the nucleus (Fig. 2C). Consistent with this finding, FISH probe hybridization combined with immunofluorescence experiments confirmed that LncRNA-Gm17586 is primarily expressed in the cytoplasm and that its expression decreases upon *S. typhimurium* infection for 4 h (Fig. 2D). These findings collectively demonstrate that *S. typhimurium* infection alters the lncRNA expression profile in RAW264.7 cells, particularly by inhibiting the expression of LncRNA-Gm17586.

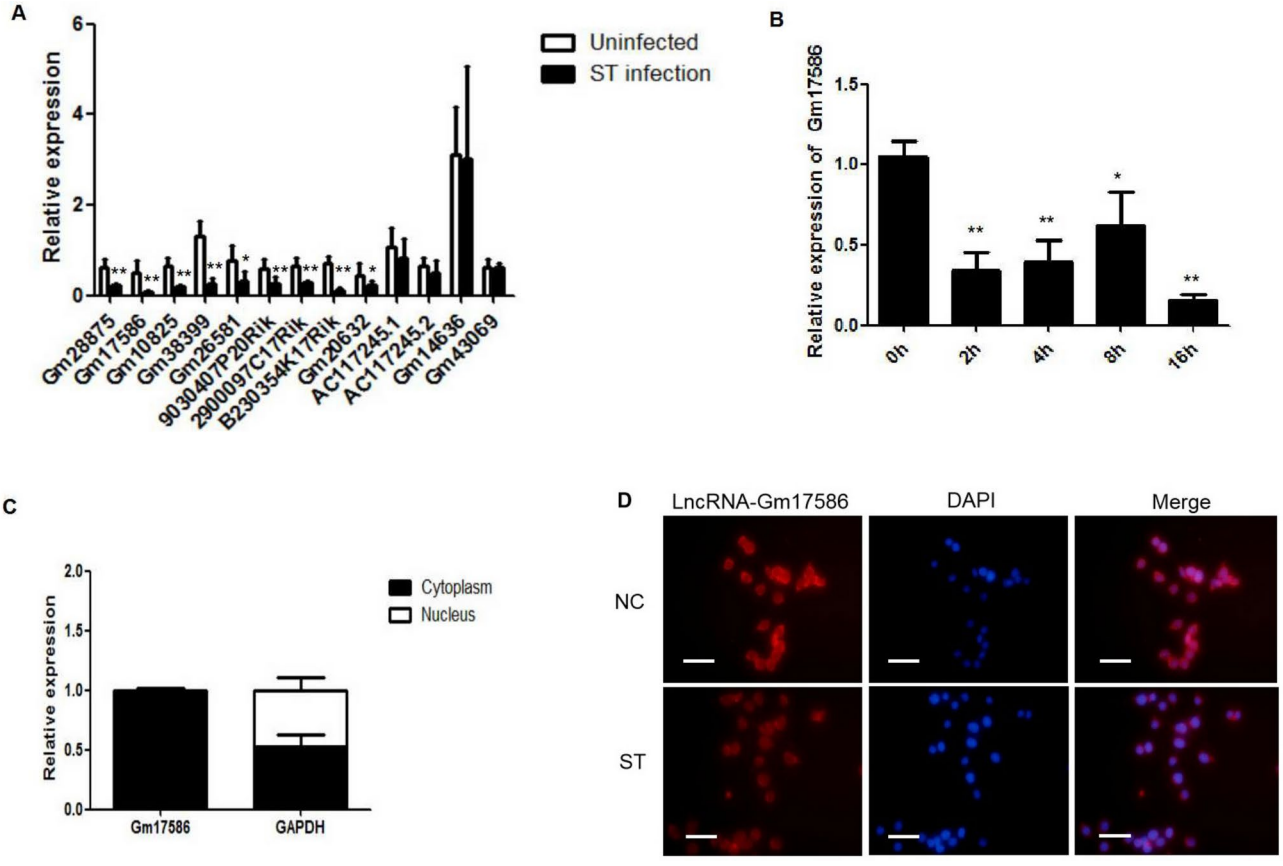

Fig. 2. Validation of Sequencing Results and Subcellular Localization of LncRNA-Gm17586. (**A**): qPCR validation of differential lncRNA expression levels in RAW264.7 cells infected with *S. typhimurium* compared to the uninfected group ($n = 3$, **$p < 0.01$ compared with the uninfected group). (**B**): Time-course qPCR analysis was performed to detect the expression levels of LncRNA-Gm17586 in RAW264.7 cells infected with *S. typhimurium* at different time points ($n = 3$, **$p < 0.01$ compared with the 0-h time point). (**C**): The cytoplasm and nucleus of RAW264.7 cells were separated, and qPCR was used to quantify the expression of LncRNA-Gm17586 in both compartments ($n = 3$). (**D**): Fluorescence in situ hybridization (FISH) was employed to visualize the subcellular localization of LncRNA-Gm17586 in RAW264.7 cells and to assess its expression level 4 h post-infection with *S. typhimurium* (Magnification, × 40). Each experiment was independently repeated three times.

LncRNA-Gm17586 inhibits S. typhimurium-induced pyroptosis in RAW264.7 Cells

To investigate the role of LncRNA-Gm17586 in *S.typhimurium*-mediated pyroptosis, we constructed a lentivirus expressing LncRNA-Gm17586 (LV-Gm17586) and infected RAW264.7 cells for 72 h. Fluorescence microscopy revealed that LncRNA-Gm17586 exhibited fluorescent expression in RAW264.7 cells after 72 h of infection. qPCR analysis confirmed that the expression of LncRNA-Gm17586 increased by 51.35-fold compared to the control group (**$p < 0.01$; Fig. 3A and 3B). Additionally, we found that overexpression of LncRNA-Gm17586 led to a significant decrease in the expression of NLRP3, caspase-1, caspase-1 p20, GSDMD, and GSDMD p30 in RAW264.7 cells, thereby inhibiting the upregulation of these proteins induced by *S. typhimurium* (**$p < 0.01$, ##$p < 0.01$; Fig. 3C and 3D). The lactate dehydrogenase (LDH) release assay demonstrated that LncRNA-Gm17586 significantly reduced LDH release caused by *S. typhimurium* infection. Furthermore, ELISA analysis of the culture supernatant and cell lysates showed that overexpression of LncRNA-Gm17586 significantly inhibited IL-1β release induced by *S. typhimurium* (**$p < 0.01$, #$p < 0.05$; Fig. 3E and 3F). These findings collectively indicate that LncRNA-Gm17586 can inhibit *S.typhimurium*-mediated pyroptosis in RAW264.7 cells, thereby reducing cellular inflammatory damage.

LncRNA-Gm17586 enhances the binding of Tnip1 and NLRP3 to inhibit S. typhimurium-induced pyroptosis

To explore the molecular mechanism by which LncRNA-Gm17586 synergistically regulates the NLRP3 inflammasome in the presence of *S. typhimurium* infection, we conducted a series of experiments. First, we infected RAW264.7 cells overexpressing LncRNA-Gm17586 with *S. typhimurium* and used immunoprecipitation (IP) technology to capture protein molecules that directly interact with NLRP3. Differential bands were visualized after SDS-PAGE and silver staining, and identified through mass spectrometry and protein sequence library searches. The results showed a significant difference in Tnip1 expression levels between the LncRNA-Gm17586 overexpression group and the co-infection group, as indicated by the red rectangular box in Fig. 4A (Fig. 4A). Furthermore, IP experiments demonstrated that the expression levels of Tnip1 and NLRP3 were significantly increased and exhibited direct interaction after 4 h of *S. typhimurium* infection in RAW264.7 cells. Overexpression of LncRNA-Gm17586 enhanced Tnip1 expression and promoted the interaction between Tnip1 and NLRP3 induced by *S. typhimurium* infection (Fig. 4B). Immunofluorescence experiments confirmed that LncRNA-Gm17586 further enhanced the interaction between Tnip1 and NLRP3 upon *S. typhimurium* infection (Fig. 4C). To demonstrate the regulatory role of Tnip1 and its co-regulatory effect with LncRNA-Gm17586 in *S. typhimurium-induced* pyroptosis, we constructed a lentivirus (LV-Tnip1) overexpressing Tnip1 and co-expressed it with LV-Gm17586 in RAW264.7 cells. The results showed that overexpression of Tnip1 significantly reduced the expression of NLRP3, caspase-1, caspase-1 p20, GSDMD, and GSDMD p30 in *S. typhimurium*-infected RAW264.7 cells (*$p < 0.05$). Moreover, co-expression of Tnip1 and LncRNA-Gm17586 further inhibited the activation of the NLRP3 inflammasome by *S. typhimurium* (#$p < 0.05$; Fig. 4D and 4E). Finally, overexpression of Tnip1 decreased the release of lactate dehydrogenase (LDH) and IL-1β in *S. typhimurium*-infected RAW264.7 cells (**$p < 0.01$). Co-expression of LncRNA-Gm17586 significantly alleviated the release of LDH and IL-1β induced by *S. typhimurium* (##$p < 0.01$; Fig. 4F and 4G). These findings collectively indicate that overexpression of LncRNA-Gm17586 enhances the binding of Tnip1 and NLRP3, thereby inhibiting *S. typhimurium*-induced pyroptosis and reducing cellular inflammatory damage.

Discussion

In this study, we identified LncRNA-Gm17586 in RAW264.7 macrophages infected with *S. typhimurium*, which directly interacts with NLRP3 inflammasome molecules. We demonstrated that its expression is significantly downregulated following *S.typhimurium* infection. Subsequently, we conducted a preliminary investigation into the functional role of LncRNA-Gm17586 and found that it can inhibit *S.typhimurium*-mediated pyroptosis in RAW264.7 macrophages. Further mechanistic studies revealed that LncRNA-Gm17586 enhances the recruitment of Tnip1 to regulate NLRP3 inflammasomes. In contrast, cells lacking LncRNA-Gm17586 exhibit insufficient Tnip1 levels to effectively control NLRP3 inflammasome activation. This deficiency may be a key factor contributing to the host inflammatory imbalance induced by *S. typhimurium*.

TNFAIP3-interacting protein 1 (Tnip1) is a protein that inhibits transmembrane receptor signaling pathways, including TNFα-R, EGFR, and TLR, as well as nuclear receptor activity, such as peroxisome proliferator-activated receptors (PPAR) and retinoic acid receptors (RAR). Deficiency or dysfunction of Tnip1 can lead to abnormal inflammatory responses, contributing to chronic inflammatory diseases[24]. Oshima et al. demonstrated that human and mouse cell lines lacking Tnip1 are susceptible to TNF-α-induced programmed cell death (PCD), while exogenous overexpression of Tnip1 restores the normal phenotype of these cells[25,26]. Additionally, Tnip1 is induced by lipopolysaccharide (LPS) in macrophages and inhibits LPS-induced inflammatory responses[27]. In our study, we found that overexpression of Tnip1 alone significantly reduces the expression of NLRP3, caspase-1, caspase-1 p20, GSDMD, and GSDMD p30 in cells. Moreover, co-expression of Tnip1 with LncRNA-Gm17586 maximizes the inhibition of *S. typhimurium*-induced pyroptosis.

lncRNAs have been proven to regulate multiple cellular functions and are involved in the pathogenesis of various infectious diseases. Pathogen infection typically modulates the expression of lncRNAs in host cells, which is crucial for the progression of pathogen infection. Additionally, the host regulates lncRNA expression or collaborates with other anti-inflammatory proteins to control pathogen infection[28-30]. Our research found that LncRNA-Gm17586 and Tnip1 exhibit anti-inflammatory effects. In uninfected RAW264.7 cells, LncRNA-Gm17586 shows high expression, while Tnip1 exhibits low expression. During this state, LncRNA-Gm17586 primarily exerts an inhibitory effect on NLRP3 inflammasomes. Upon *S.typhimurium* infection, LncRNA-Gm17586 expression decreases, leading to NLRP3 inflammasome activation. At this point, cells mobilize Tnip1 to inhibit overactivated NLRP3 inflammasomes, potentially as a negative feedback mechanism to regulate

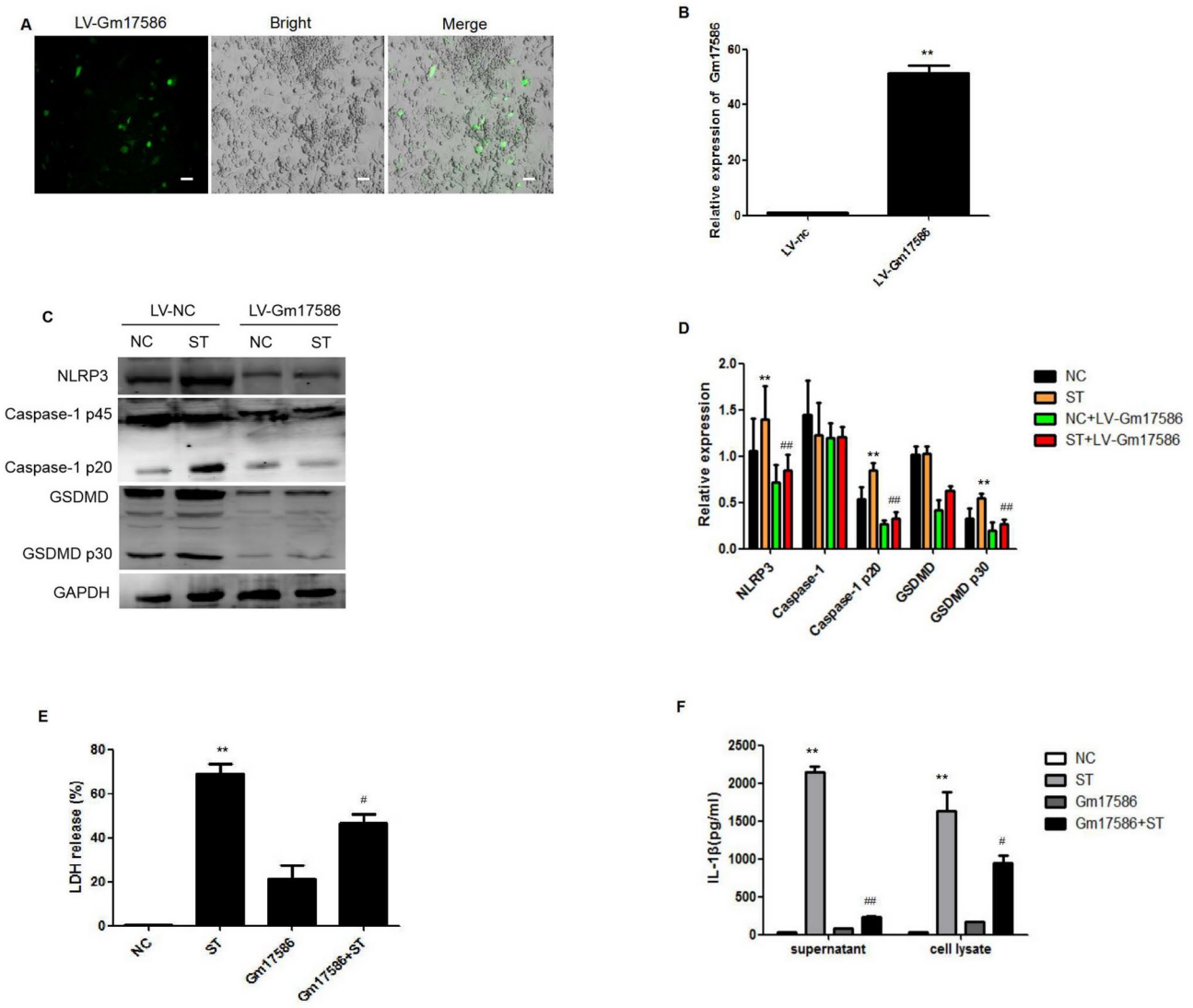

Fig. 3. **LncRNA-Gm17586 Inhibits S.typhimurium-Mediated Pyroptosis in RAW264.7 Cells.** (**A**): We constructed a lentivirus overexpressing LncRNA-Gm17586 and infected RAW264.7 cells at an MOI of 10. Green fluorescence expression was observed at 72 h post-infection (magnification, × 20). Each experiment was independently repeated three times. (**B**): After 72 h of lentiviral infection, qPCR was used to detect the expression level of LncRNA-Gm17586. The results showed significant upregulation compared to the LV-nc group (**$p < 0.01$). Each experiment was independently repeated three times. (**C**): Following 72 h of LncRNA-Gm17586 overexpression and subsequent infection of RAW264.7 cells with *S. typhimurium* at an MOI of 20 for 4 h, cell lysates were collected. Western blotting was performed to detect the expression levels of NLRP3, caspase-1, caspase-1 p20, GSDMD, and GSDMD p30. Each experiment was independently repeated three times. (**D**): Statistical analysis revealed that the expression levels of NLRP3, caspase-1, caspase-1 p20, GSDMD, and GSDMD p30 were significantly reduced in the LncRNA-Gm17586 overexpression group compared to the NC group (**$p < 0.01$) or the ST group (##$p < 0.01$). (**E**): After 72 h of LncRNA-Gm17586 overexpression, cells were infected with *S. typhimurium* at an MOI of 20 for 4 h. LDH release was measured using a lactate dehydrogenase cytotoxicity assay kit. Results showed significant reduction in LDH release compared to the NC group (**$p < 0.01$) or the ST group (#$p < 0.05$). Each experiment was independently repeated three times. (**F**): After 72 h of LncRNA-Gm17586 overexpression, cells were infected with *S. typhimurium* at an MOI of 20 for 4 h. The cell supernatant was collected, and IL-1β levels were detected using ELISA. Results showed significant reduction in IL-1β levels compared to the NC group (*$p < 0.05$), the ST group (##$p < 0.01$), or the ST group (#$p < 0.05$). Each experiment was independently repeated three times.

inflammation. However, the reduced expression of LncRNA-Gm17586 caused by *S.typhimurium* impairs its inhibitory effect on NLRP3 inflammasomes. Without the assistance of LncRNA-Gm17586, even high levels of Tnip1 cannot effectively inhibit the expression of NLRP3 inflammasome-related proteins, resulting in sustained inflammation. When LncRNA-Gm17586 is overexpressed, it directly interacts with NLRP3, leading to decreased NLRP3 expression. Consequently, cells do not need to express excessive Tnip1 to maintain the

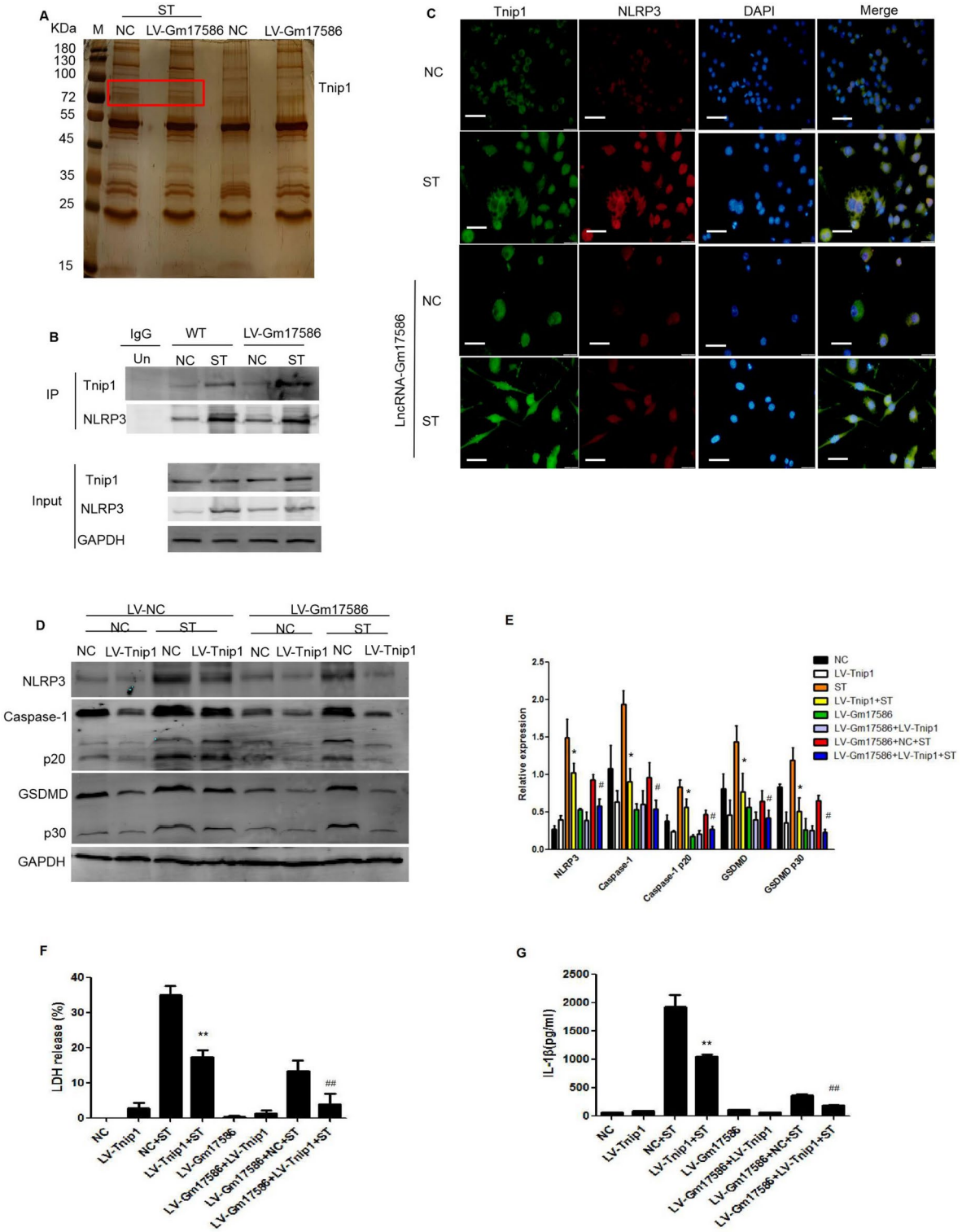

inflammatory response within a reasonable range. When LncRNA-Gm17586 is overexpressed in cells infected with *S.typhimurium*, it not only inhibits NLRP3 but also recruits more Tnip1 to bind to NLRP3, enhancing their binding affinity. This dual interaction exerts a synergistic inhibitory effect on NLRP3 (Fig. 5). We conclude that LncRNA-Gm17586 acts as both a primary inhibitor of NLRP3 activation and a co-factor for Tnip1, synergistically suppressing NLRP3 activation and playing a dual role in *S.typhimurium*-mediated pyroptosis.

This study identified long non-coding RNA-Gm17586 as a key regulatory factor of the inflammatory response in macrophages infected with *S.typhimurium* and analyzed its physiological and pathological functions in inhibiting the NLRP3 inflammasome-mediated innate immune response, making a positive contribution to further revealing the function of the LncRNA-Gm17586 molecule. However, this study has limitations, as lncRNA-Gm17586 is a mouse-specific long non-coding RNA with no homologous genes in other species, which may limit the direct applicability of our findings to other species. In the future, we propose generating

◂**Fig. 4. LncRNA-Gm17586 Enhances Tnip1 Binding to NLRP3 to Inhibit S. typhimurium-Mediated Pyroptosis.** (**A**): RAW264.7 cells overexpressing LncRNA-Gm17586 for 72 h were infected with *S. typhimurium* at an MOI of 20 for 4 h. Cell lysates were immunoprecipitated using an NLRP3-specific primary antibody, and silver-stained gel strips were obtained by SDS-PAGE electrophoresis. Each experiment was independently repeated three times. (**B**): After 72 h of LncRNA-Gm17586 overexpression, RAW264.7 cells were infected with *S. typhimurium* at an MOI of 20 for 4 h. Co-immunoprecipitation (Co-IP) was performed using an NLRP3-specific primary antibody to detect the interaction between NLRP3 and Tnip1. Each experiment was independently repeated three times. (**C**): RAW264.7 cells overexpressing LncRNA-Gm17586 for 72 h were either left uninfected or infected with *S. typhimurium* at an MOI of 20 for 4 h. Immunofluorescence assays were used to detect the expression levels and co-localization of NLRP3 and Tnip1 (Magnification × 40). Each experiment was independently repeated three times. (**D**): RAW264.7 cells were transfected with lentiviruses overexpressing LncRNA-Gm17586 or Tnip1, or both genes simultaneously. After 72 h, cells were infected with *S. typhimurium* at an MOI of 20 for 4 h. Western blotting was performed to detect the expression levels of NLRP3, caspase-1, caspase-1 p20, GSDMD, and GSDMD p30. Each experiment was independently repeated three times. (**E**): Statistical analysis revealed that the expression levels of NLRP3, caspase-1, caspase-1 p20, GSDMD, and GSDMD p30 were significantly reduced in the LncRNA-Gm17586 overexpression group compared to the ST group (*$p < 0.05$) or the Lv-Gm17586 + NC + ST group (#$p < 0.05$). (**F**): RAW264.7 cells were transfected with lentiviruses overexpressing LncRNA-Gm17586 or Tnip1, or both genes simultaneously. After 72 h, cells were infected with *S. typhimurium* at an MOI of 20 for 4 h. LDH release was measured using a lactate dehydrogenase cytotoxicity assay kit. Results showed significant reduction in LDH release compared to the NC + ST group (**$p < 0.01$) or the Lv-Gm17586 + NC + ST group (##$p < 0.01$). Each experiment was independently repeated three times. (**G**): RAW264.7 cells were transfected with lentiviruses overexpressing LncRNA-Gm17586 or Tnip1, or both genes simultaneously. After 72 h, cells were infected with *S. typhimurium* at an MOI of 20 for 4 h. The release of IL-1β in the cell supernatant was detected by ELISA. Results showed significant reduction in IL-1β levels compared to the NC + ST group (**$p < 0.01$) or the Lv-Gm17586 + NC + ST group (##$p < 0.01$). Each experiment was independently repeated three times.

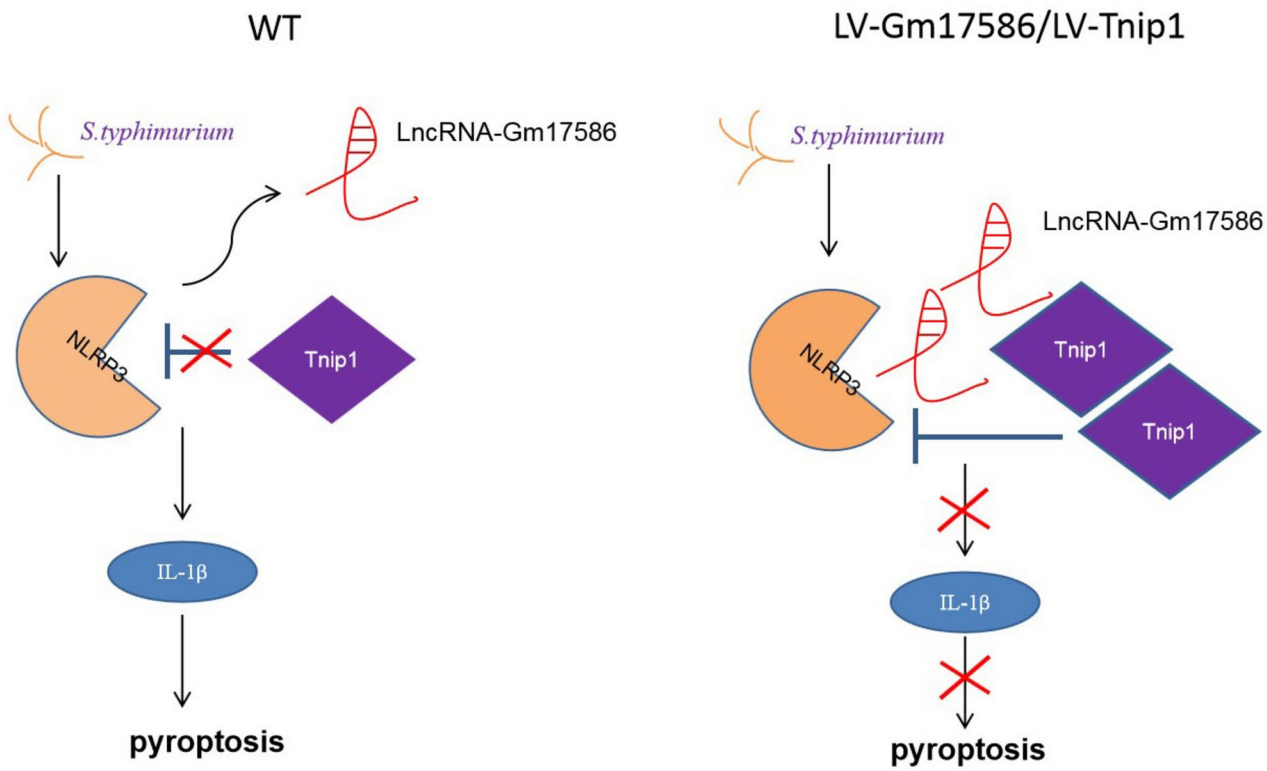

Fig. 5. Schematic Model of the Proposed Mechanisms. In wild-type RAW264.7 cells infected with *S.typhimurium*, the expression of LncRNA-Gm17586 is downregulated, leading to a loss of control over NLRP3 activation. In response, cells upregulate Tnip1 expression as a feedback mechanism to balance the inflammatory response. However, in the absence of LncRNA-Gm17586, Tnip1 alone cannot fully inhibit NLRP3, resulting in uncontrolled pyroptosis mediated by *S. typhimurium*. When RAW264.7 cells overexpressing LncRNA-Gm17586 are infected with *S. typhimurium*, the increased levels of LncRNA-Gm17586 re-establish its interaction with NLRP3, thereby inhibiting NLRP3 expression. Moreover, elevated LncRNA-Gm17586 recruits additional Tnip1 and enhances its binding affinity to NLRP3, further suppressing *S.typhimurium*-mediated pyroptosis.

mutant mice lacking lncRNA-Gm17586 to further investigate its unknown functions. This approach will allow us to comprehensively elucidate the physiological and pathological roles of lncRNA-Gm17586 in these mice. Additionally, we hope that such studies will contribute to the development of new gene therapy tools as technology advances, ultimately aiding the scientific community in addressing inflammatory diseases.

Data availability

The data supporting the findings of this study are openly available in Figshare at https://figshare.com/s/e5249c3e9c7aea9f1aa6 and sequencing data were deposited in the National Center for Biotechnology Information Gene Expression Omnibus database (GSE-250407), https://www.ncbi.nlm.nih.gov/geo/query/acc.cgi?acc=GSE250407.

Received: 5 December 2024; Accepted: 19 February 2025
Published online: 25 February 2025

References

1. Sun, H. et al. The epidemiology of monophasic *Salmonella* typhimurium. *Foodborne Pathog. Dis.* **17**(2), 87–97 (2020).
2. Dos Santos, A. M. P., Ferrari, R. G. & Junior Conte, C. A. Virulence factors in S. typhimurium: The sagacity of a bacterium. *Curr. Microbiol.* **76**(6), 762–773 (2019).
3. Broz, P, Ohlson, M. B. & Monack, D. M. Innate immune response to S.typhimurium, a model enteric pathogen. *Gut Microbes.* **3**(2), 62-70 (2012).
4. Kim, J.-J. & Jo, E. -K. The NLRP3 inflammasome and host protection against bacterial infection. *J Korean Med Sci*. **28**(10), 1415-23 (2013).
5. Zhao, C & Zhao, W. NLRP3 inflammasome A plays a key role in antiviral response. *Front Immunol.* **11**, 211 (2020).
6. Zhen, Y. & Zhang, H. NLRP3 inflammasomes and inflammatory bowel disease. *Front Immunol.* **10**, 276 (2019).
7. Holbrook, J. A. et al. Neurodegenerative Disease and the NLRP3 Inflammasome. Front Pharmacol 12, 643254 (2021).
8. Lili, Yu. et al. NLRP3 Inflammasome in Non-Alcoholic Fatty Liver Disease and Steatohepatitis: Therapeutic Targets and Treatment. *Front Pharmacol*. **13**, 780496 (2022).
9. Sharma, B, R. & Kanneganti, T, D. NLRP3 Inflammasomes in Cancer and Metabolic Diseases. *Nat Immunol*. **22**(5), 550-59 (2021).
10. Jianing, Fu & Hao, Wu. Structural Mechanisms of NLRP3 Inflammasome Assembly and Activation. *Annu Rev Immunol* **41**, 301-16 (2023).
11. Clare, B. Inflammasome Activation by Salmonella. *Curr Opin Microbiol.* **64**, 27-32 (2021).
12. Broz, P. et al. Redundant roles of inflammasome receptors NLRP3 and NLRC4 in the host defense against Salmonella. *J. Exp. Med* **207**, 1745-55 (2010).
13. Gram, A. M. et al. Salmonella flagellin activates NAIP/NLRC4 and canonical NLRP3 inflammasome in human macrophages. *J. Immunol.* **206**, 631-40 (2021).
14. Robinson, E. K., Covarrubias, S & Carpenter, S. How and why lncRNAs function is an innate immune perspective. *Biochim Biophys Acta Gene Regul Mech.* **1863**, 194419 (2020).
15. Fernandes J. C. R. et al. lncRNAs in the regulation of gene expression: physiology and disease. *Noncoding RNA*. **5**, 17 (2019).
16. Batista, P. J & Chang, H. Y. Long non-coding RNAs: Cellular address codes in development and disease. *Cell*. **152**, 1298–307 (2013).
17. Feng, X. et al. Non-coding RNAs: key regulators of NLRP3 inflammasome-mediated inflammatory diseases. *Int Immunopharmacol.* **100**, 108105 (2021).
18. Al-Hawary, S. I.S. et al. The NLRP3 inflammasome pathway in atherosclerosis: Focusing on the therapeutic potential of non-coding RNAs. *Pathol Res Pract.* **246**, 154490 (2023).
19. Xiaolin, Lu. et al. Emerging Role of LncRNA Regulation for NLRP3 Inflammasome in Diabetes Complications. *Front Cell Dev Biol.* **9**, 792401 (2022).
20. Niu, B. et al. lncRNA KCNQ1OT1 promotes hepatitis C virus-induced pyroptosis of β-cells by mediating the miR-223-3p/NLRP3 axis. *Ann Transl Med.* **9**(17), 1387 (2021).
21. Deng, X. et al. Brucella-Induced Downregulation of lncRNA Gm28309 triggers the macrophage inflammatory response through the miR-3068-5p/NF-κB Pathway. *Front Immunol* **11**, 581517 (2020).
22. Zou, W. et al. Asiatic acid attenuates Salmonella induced inflammation by Salmonella via upregulation of lncRNA TVX1 in microglia. *Int J Mol Sci.* **23**(18), 10978 (2022).
23. Tan, S. et al. Chlorogenic Acid Promotes Autophagy and Alleviates Salmonella Typhimurium Infection Through lncRNAGAS5/miR-23a/PTEN axis and p38 MAPK Pathway. *Front Cell Dev Biol* **8**, 552020 (2020).
24. Ramirez, V. P., Gurevich, I. & Aneskievieh, B. J. Emerging roles of TNIP1 in regulating post-receptor signaling. *Cytokine Growth Factor Rev.* **23**(3), 109-18 (2012).
25. Oshima, S. et al. ABIN-1 is a ubiquitin sensor that restricts cell death and promotes embryonic development. *Nature*. **457**, 906–9 (2009).
26. Guicciardi, M. E & Gores, G. J. Life and death by death receptors. FASEB J. 23, 1625–37 (2009).
27. Wullaert, A. et al. LIND/ABIN-3 is a novel lipopolysaccharide-inducible inhibitor of NF-κB activation. *J Biol Chem.* **282**(1), 81-90 (2007).
28. Shen, Li. et al. Roles and potential applications of lncRNAs in HIV infection. *Int J Infect Dis.* **92**, 97-104 (2020).
29. Yi, K. et al. Longnon-coding RNA and its role in viral infection and pathogenesis. *Front Biosci (Landmark Ed).* **24**(4), 777-789 (2019).
30. Qiu, Li. et al. Long Non-coding RNAs: Regulators of Viral Infection and the Interferon Antiviral Response. *Front Microbiol.* **9**, 1621 (2018).

Author contributions

Concept and design: Zhiyuan An, data collection and analysis: Wenyi Ding, drafting of the article: Zhiyuan An and Wenyi Ding, study supervision: Zhiyuan An. All the author approved the final article.

Funding

This study was supported by the National Natural Science Foundation of China (Grant No. 81900074).

Declarations

Competing interests
The authors declare no competing interests.

Additional information
Supplementary Information The online version contains supplementary material available at https://doi.org/10.1038/s41598-025-91296-2.

Correspondence and requests for materials should be addressed to Z.A.

Reprints and permissions information is available at www.nature.com/reprints.

Publisher's note Springer Nature remains neutral with regard to jurisdictional claims in published maps and institutional affiliations.

Open Access This article is licensed under a Creative Commons Attribution-NonCommercial-NoDerivatives 4.0 International License, which permits any non-commercial use, sharing, distribution and reproduction in any medium or format, as long as you give appropriate credit to the original author(s) and the source, provide a link to the Creative Commons licence, and indicate if you modified the licensed material. You do not have permission under this licence to share adapted material derived from this article or parts of it. The images or other third party material in this article are included in the article's Creative Commons licence, unless indicated otherwise in a credit line to the material. If material is not included in the article's Creative Commons licence and your intended use is not permitted by statutory regulation or exceeds the permitted use, you will need to obtain permission directly from the copyright holder. To view a copy of this licence, visit http://creativecommons.org/licenses/by-nc-nd/4.0/.

© The Author(s) 2025